

Hvor er polarfronten?

Barents Sea Exploration Collaboration (BaSEC) er et industrisamarbeid for å forberede leteoperasjoner i Barentshavet. BaSECs siktemål er å koordinere og komme med anbefalinger om tiltak som kan danne grunnlag for sikker og effektiv letevirsomhet i Barentshavet. BaSEC har 17 medlemmer, alle aktiv på norsk sokkel. BaSEC bygger sine rapporter på beste tilgjengelige kunnskap og på den brede erfaring disse 17 selskapene har fra operasjoner på norsk sokkel og i andre områder med tilsvarende forhold.

Et av de viktigste særskilt verdifulle områdene (SVO) i Barentshavet er polarfronten, som utgjør sonen der varmt vann fra sør møter kaldt vann fra nord. I likhet med iskanten ble den forsøkt definert og fastlagt i forvaltningsplanen for Lofoten, Vesterålen, Senja og Barentshavet (heretter forvaltningsplanen) fra 2010. Denne definisjonen har vært retningsgivende for forvaltning av disse havområdene i perioden etter.

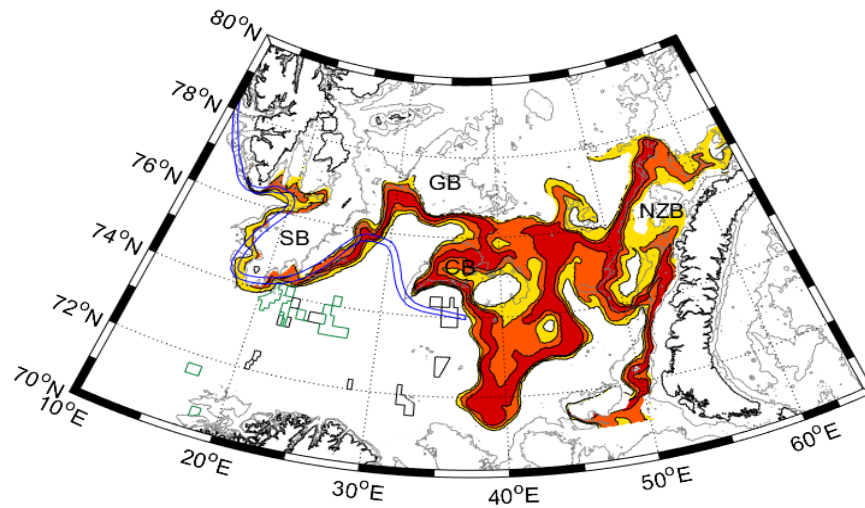
For å kunne ha best mulig grunnlag for den risikobaserte forvaltning av ressursene og for å kunne best mulig forstå risikoen knyttet til leteaktivitet i Barentshavet, har BaSEC sett nærmere på lokaliseringen av polarfronten.

Basert på validerte modelldata over de siste 57 årene

Basert på et datasett (SVIM-modellarkivet utarbeidet av Havforskningsinstituttet) som strekker seg over 57 år (1960-2016) gir rapporten en mer presis og oppdatert forståelse av hvor polarfronten er og hvor stabil den er. SVIM-modellarkivet er offentlig tilgjengelig, og sammen med de to datasettene resultatene er evaluert mot, representerer dette et svært godt datagrunnlag. Fronten er identifisert ved hjelp av en publisert metode som tar utgangspunkt i å finne den vanligste temperaturen i områder med brå temperaturovergang (50-100 m dyp). Studiet av havtemperaturen i SVIM gir et godt utgangspunkt for en oppdatert forståelse av det fysiske fenomenet polarfronten.

Polarfronten følger topografien på havbunnen

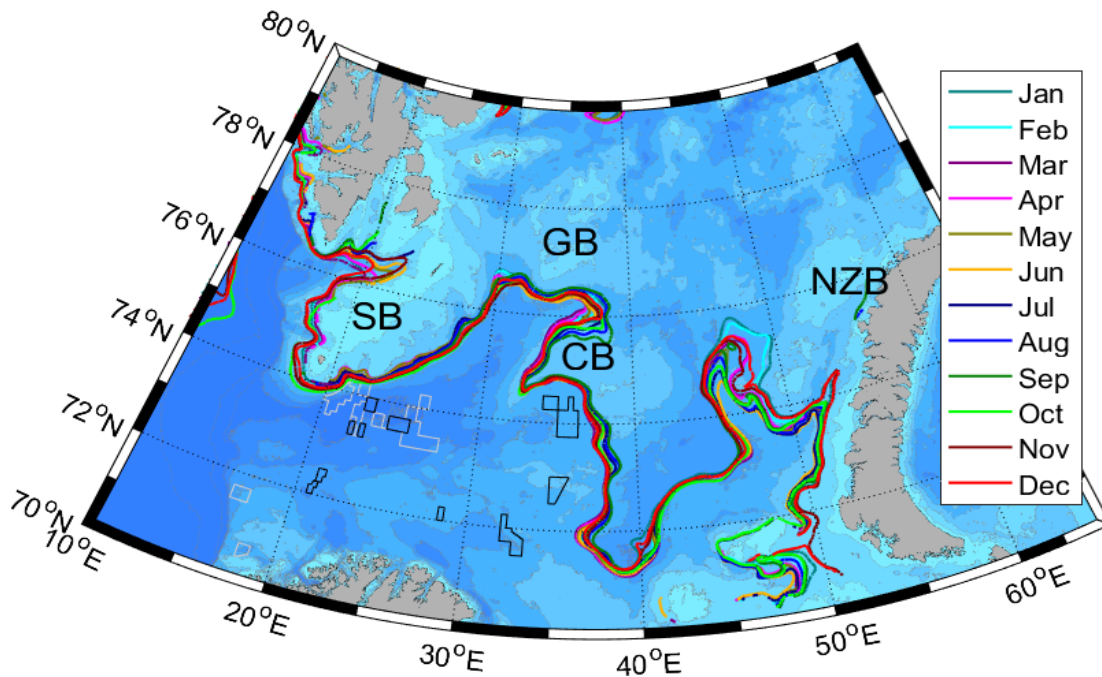
Analysen viser at polarfronten følger topografien på havbunnen. Det betyr at den følger sørsiden av Spitsbergenbanken, Storbanken, Sentralbanken og Novaja Semlja-banken. Deler av dette er lenger nord enn det som angis i forvaltningsplanen. I illustrasjonen nedenfor ser man betydningen av dette. Det impliserer at polarfronten stort sett følger den opptegnede linjen fra forvaltningsplanen frem til 30° Ø. Øst for 30° Ø viser analysen at polarfronten ligger lenger nord enn det forvaltningsplanen angir og nord for de områdene som i dag er åpne for olje- og gassvirksomhet. Øst for norske territorialfarvann, på russisk side er polarfronten mer variert.



10 (gul), 50 (oransje), og 90 (rød) persentilen for lokalisering av polarfronten SB - Spitsbergenbanken, GB - Storbanken, CB - Sentralbanken og NZB - Novaja Semlja-banken. Forvaltningsplanens omriss av polarfronten i blått.

Polarfronten er stabil

Analysen viser at posisjonen til polarfronten varierer lite gjennom året. Figuren nedenfor viser hvor den sørligste posisjonen for fronten normalt ligger for hver måned av året.



Rapporten finner også at polarfronten er stabil over tid. Det er små variasjoner i posisjonen til fronten fra 1960 og fram til i dag. I løpet av denne perioden har det vært en temperaturstigning på omtrent 1 grad Celsius i havtemperaturen som karakteriserer fronten.

Rapporten undersøker også hvordan polarfrontens lokalisering varierer med havdypet. Analysen viser at den sørligste posisjonen er lik, men at fronten som er identifisert i overflatelaget (0-20m) vandrer lenger nordover i sommermånedene.

Polarfronten ligger nord og øst for Korp fjell

I forvaltningsplanen er det angitt at polarfronten går tvers gjennom utvinningstillatelsen PL859, også kjent som Korp fjell. Dette samsvarer ikke med analysen som foreligger her, som har identifisert fronten langs topografien nord og øst for Korp fjell. Den korteste avstanden fra brønnlokasjonen for Korp fjell Deep til polarfronten er typisk 40 km i vintermånedene og øker til typisk 50 km om sommeren.

Statistical position of the oceanic polar front in the Barents Sea

MAD-RE2018-016

Title: Statistical position of the oceanic polar front in the Barents Sea		
Document no MAD-RE2018-016	Contract no	Project TDI Oceanographic Polar Front Study

Classification: Open	Distribution
Expiry date	Status: Final

Distribution date 2018-08-29	Rev no 0	Copy no
--	--------------------	---------

Author(s)/Source(s) Ingrid Husøy Onarheim, Sigurd Henrik Teigen	
Subjects Polar front, Barents Sea, oceanography, climate	
Remarks	
Valid from	Updated
Responsible publisher	Authority to approve deviations

Prepared by (Organisation unit / Name) Ingrid Husøy Onarheim (TPD R&T FT MMT MAD)	Date/Signature 29/8-18 X <u>Ingrid Husøy Onarheim</u>
Responsible (Organisation unit/ Name) Sigurd Henrik Teigen (TPD R&T FT MMT MAD)	Date/Signature 29/8-18 X <u>Sigurd H. Teigen</u>
Recommended (Organisation unit/ Name) Kenneth Johannessen Eik (TPD R&T FT MMT MAD)	Date/Signature 29/8-18 X <u>K. J. Eik</u>
Approved by (Organisation unit/ Name) Jens Christian Roth (TPD R&T FT MMT MAD)	Date/Signature 29/8-18 X <u>Jens Christian Roth</u>

Table of contents

1	Executive summary	4
2	Introduction	5
3	Data and methods	6
3.1	Modified Oziel et al. (2016)	7
4	Results	9
4.1	Position of physical polar front	9
4.1.1	Seasonal variability and long-term change	9
4.1.2	Surface polar front	12
4.2	Validation	13
4.2.1	Comparison with NSA	13
4.2.2	Comparison with BaSIC4	14
5	Summary and conclusions	15
6	References	15

1 Executive summary

The Barents Sea Polar Front (PF) is an oceanic feature that separates warm and saline Atlantic water in the south from cold and fresh Arctic water in the north. In the western Barents Sea, the PF is tied to the bathymetry, whereas the front is typically less distinct and less studied further east. The numerical ocean model hindcast archive SVIM (Lien et al., 2013) is herein used to assess the position and variability of the PF at 50-100 m depth between 1960 and 2016 on a 4x4 km grid. Based on probability density functions, we find that the PF largely follows the bathymetry (Figure 1) and has limited seasonal and interannual variations (Figure 5), except for near the Novaya Zemlya Bank. The position of the front agrees well with the front outlined in the management plan (Ministry of Climate and Environment, 2011) west of 30°E, whereas further east we find that the topographic control persists, contrasting the front in the management plan. With particular emphasis on the planned well 7335/3-1 in license PL859, we find that the shortest distance to the PF ranges from 38 km (March) to 51 km (August and September). The distance is shortest in winter, whereas largest variability is found in summer. Overall, the position of the PF near PL859 displays a slight northeastward trend (2 km/decade) in winter and spring since 1960. The climatological position of the PF is supported by results from a climatological atlas of the Nordic Seas (1960-2012; Korablev et al., 2014), and the ocean hindcast BaSIC4 (1982-2012; Røed et al., 2015).

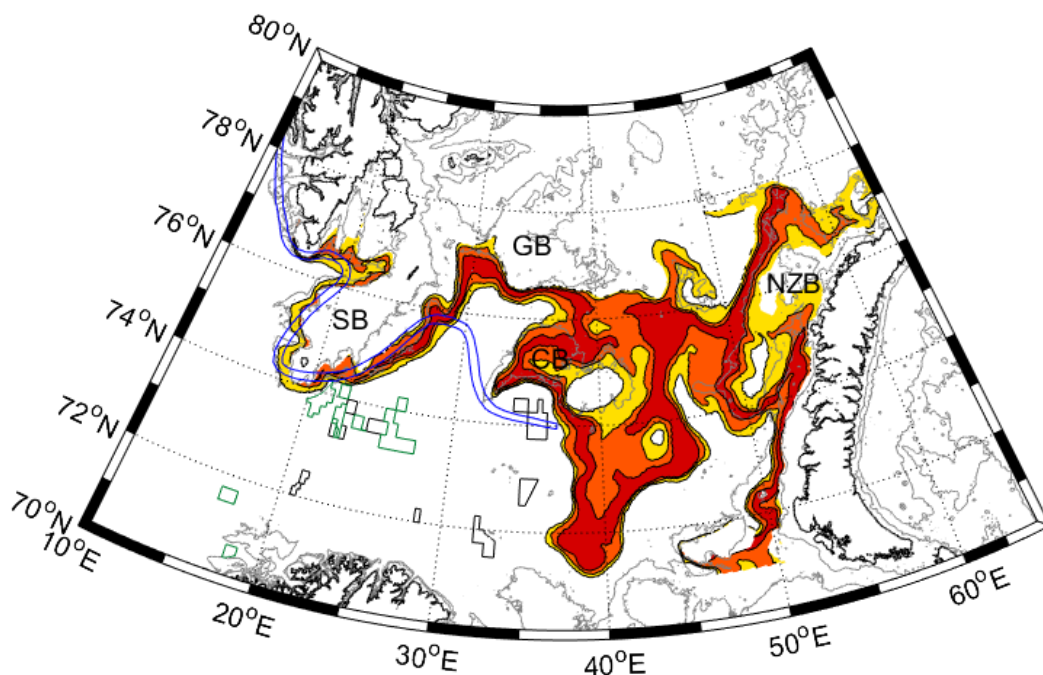


Figure 1: The 10 (yellow), 50 (orange), and 90 (red) percentiles for the location of the PF in the 57-year SVIM archive. The PF as defined in the management plan (blue), licenses awarded in the 23rd (black) and 24th (green) concession round, and the 100-m and 200-m isobaths (grey) are shown. Abbreviations are SB: Spitsbergen Bank, CB: Central Bank, GB: Great Bank, NZB: Novaya Zemlya Bank.

2 Introduction

The Barents Sea is a shallow continental shelf sea with four prominent banks; the Spitsbergen Bank, Central Bank, Great Bank, and Novaya Zemlya Bank (Figure 2), and an average depth of 230 m. Warm and saline Atlantic water enters the Barents Sea in the southwest (Ingvaldsen et al., 2004), and after substantial water mass transformation, modified Atlantic water exits the Barents Sea in the northeast (Gammelsrød et al., 2009). Cold and fresh water of Arctic origin enters the Barents Sea from the north, between Svalbard and Franz Josef Land, and between Frans Josef Land and Novaya Zemlya, and dominates the northern Barents Sea (Midttun & Loeng, 1986). The Atlantic water in the south and the Arctic water in the north are separated by the Barents Sea Polar Front (PF); the main hydrographic feature of the upper waters in the Barents Sea (Loeng, 1991). The PF is associated with strong horizontal temperature and salinity gradients, but weak density gradients (Drinkwater & Tande, 2013). It is sharp and tied to the bathymetry in the western Barents Sea (Johannessen & Foster, 1978), but is typically broader and less distinct further east, where observations are generally sparse (Midttun & Loeng, 1986). Oziel et al. (2016) describe two fronts east of 30°E; a northern front identified by salinity gradients, and a southern front identified by temperature gradients. The southern (temperature gradient) front agrees well with the front presented by Loeng (1991).

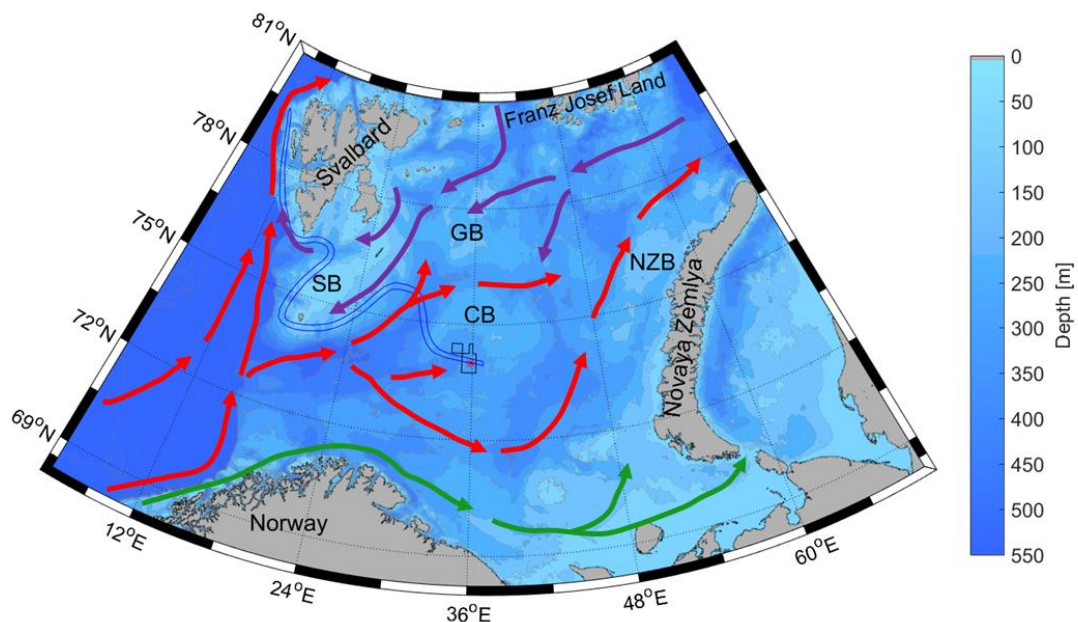


Figure 2: Bathymetric map of the Barents Sea including schematic ocean circulation with warm Atlantic water (red), cold Arctic water (purple), and the coastal current (green). License PL859 is indicated in black with well 7335/3-1 as a red star, and the PF as defined in the management plan is shown in blue. Abbreviations are SB: Spitsbergen Bank, CB: Central Bank, GB: Great Bank, NZB: Novaya Zemlya Bank.

The Barents Sea PF is defined as a “særlig verdifullt og sårbart område” (SVO) by the Ministry of Climate and Environment (2006) as the region “har vesentlig betydning for det biologiske mangfoldet og den biologiske produksjonen, og der mulige skadevirkninger kan få langvarige eller irreversible konsekvenser”. The position of the PF as defined by the management plan (positions available from <https://kartkatalog.miljodirektoratet.no/Dataset/Details/702>), intersects with license PL859 awarded to Equinor in the 23rd concession round (Figure 2).

Here we examine the spatial and temporal variability of the physical PF in the Barents Sea, with particular emphasis on the planned well 7335/3-1 in license PL859 (Korpfjell Deep), henceforth Korpfjell (74° 00' N, 35° 50' E; Statoil ASA, 2018). We focus on the front closest to our area of interest, i.e., the southern front in the Barents Sea. We note again that the southern front is defined by strong horizontal temperature gradients (Oziel et al., 2016), and we accordingly consider temperature gradients rather than salinity gradients when examining the PF. We also note that in agreement with Oziel et al. (2016), we find that the fronts defined by temperature and salinity gradients align around the Spitsbergen Bank and Great Bank, whereas further east, the salinity front turns north and the temperature front turns south.

3 Data and methods

To investigate the Barents Sea PF, we examine hydrographic data from a 57 year (1960-2016) numerical ocean model hindcast archive (SVIM), covering the Nordic and Barents Seas at a spatial resolution of 4 km (Lien et al., 2013). The hindcast employs the Regional Ocean Modeling System (ROMS; Shchepetkin & McWilliams, 2005); a three-dimensional baroclinic ocean general circulation model that uses topography-following s-coordinates in the vertical (32 sigma layers). The model is coupled to an ice module (Budgell, 2005). The 10-km-resolution Norwegian Reanalysis (NORA10) hindcast archive for the Nordic Seas (Reistad et al., 2011) is applied as atmospheric forcing. SVIM is run and regularly updated by the Institute of Marine Research, Norway, and the hindcast is freely available from Norwegian Meteorological Institute's data server (MET Norway Thredds Service, 2017). The model shows good agreement with observations, in general, and in particular with the position of the PF (Lien et al., 2013). Both the hydrographic structure, ocean transports, and sea ice cover are realistic (Lien et al., 2013). Accordingly, the SVIM archive seems appropriate to examine the structure and variability of the PF. For a more detailed description of the dataset, see Lien et al. (2013) and references therein.

We use the method proposed by Oziel et al. (2016) as a basis for determining the position of the Barents Sea PF. Based on probability density functions (PDFs), their algorithm allows for an objective estimate of the position of the front. For each timestep, the method calculates horizontal temperature gradients at 50-100 m depth (by centered differences; $gradient = \sqrt{gradient_x^2 + gradient_y^2}$, where $gradient_x$ and $gradient_y$ are the temperature gradients in the x and y directions, respectively). The 50-100 m depth interval is considered to avoid the surface layer which is directly influenced by the atmosphere, and the deeper layers where the tidally generated turbulence and mixing are strong (Parsons et al., 1996), and may weaken the gradients. Next, all grid points within 10-65°E, 70-80°N where the horizontal temperature gradient exceeds a certain threshold are identified. A PDF of the temperature of these grid points is created, and the maximum of the PDF (the modal temperature), T_m , is determined. Note that the temperature distribution is typically skewed (Figure 4b), and that the modal temperature represents the most common temperature of the grid points with gradients above the threshold. The frontal zone is thereafter defined as the area (i.e., all grid points) within the isotherms $T_m - s/2$ and $T_m + s/2$, where s is the standard deviation of the PDF (i.e., a measure of the temperature spread). This region comprises the area where it is most likely to find temperature gradients exceeding the initial threshold. Note that the method identifies the PF by temperatures associated with strong temperature gradients, rather than by the gradients directly. Oziel et al. (2016) consider a temperature gradient threshold of 0.1°C/km.

3.1 Modified Oziel et al. (2016)

Horizontal temperature gradients in the SVIM archive are not often larger than $0.1^{\circ}\text{C}/\text{km}$, neither for summer values (not shown), nor for annual means (Figure 3a), i.e., they are smaller than those presented by Oziel et al. (2016). Oziel et al. (2016) merged two observation based data sets to develop a new $0.5^{\circ} \times 0.25^{\circ}$ (latitude-longitude) summer (August-September) database for the Barents Sea. The new database is similar to the “Climatological Atlas of the Nordic Seas and Northern North Atlantic” (NSA; Korabev et al., 2014) but has generally less smooth fields than the NSA observations, partly due to different interpolation techniques (Oziel et al., 2016). We find that the annual mean values in the NSA observations and the annual means and summer means in the SVIM archive have generally smaller temperature gradients than those obtained by Oziel et al. (2016). Gradients are similar, but enhanced, in the SVIM archive relative to the NSA observations (Figure 3). This agrees well with Lien et al. (2013) who assess summer gradients, 1980-2009, and find that gradients are realistically reproduced by SVIM, but that simulated gradients appear stronger due to higher spatial resolution. The magnitude of the SVIM gradients are thus in between the trends in the two observation based datasets.

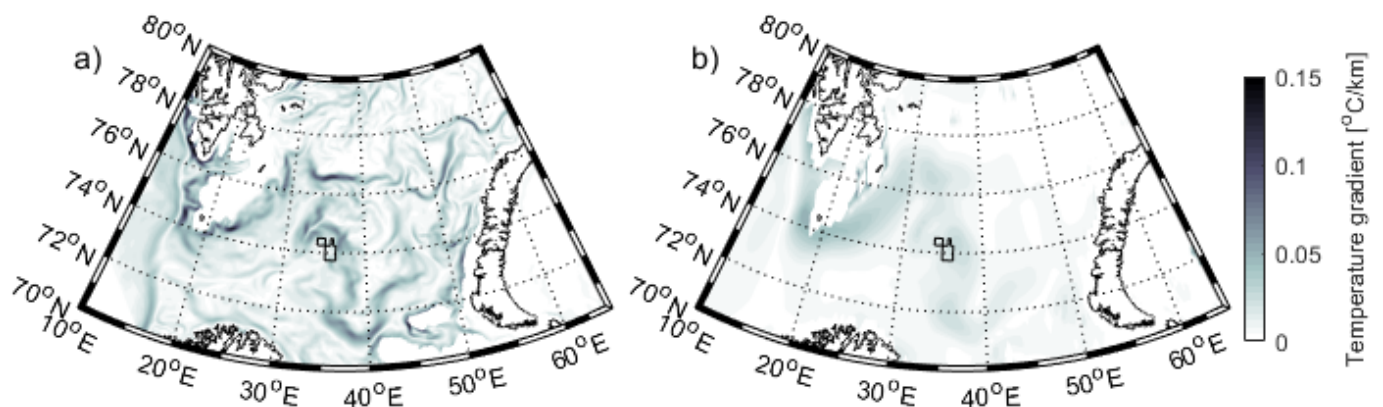


Figure 3: Average horizontal temperature gradients in SVIM (a) and NSA (b) for all months between 1960 and 2012. License PL859 is shown in black.

As temperature gradients in both SVIM and NSA are weaker than those presented by Oziel et al. (2016), we relax Oziel et al. (2016)’s temperature gradient threshold to $0.05^{\circ}\text{C}/\text{km}$. To allow for various water masses being present, we moreover, restrict our study area to grid points that at least once within the hindcast period have temperatures between 0.5°C and 3.5°C (see white contour in Figure 4a). Fronts are otherwise identified by Oziel et al. (2016)’s approach. The identified August-September frontal temperature in SVIM is the same as found by Oziel ($T_m = 0.8^{\circ}\text{C}$). By considering the complete SVIM archive (all months), $T_m = 0.6^{\circ}\text{C}$, and we find that T_m is not sensitive to small changes in the temperature gradient criteria, particularly for stronger gradients (Table 1). Note that the number of grid points gradually drops for stronger temperature gradients. For temperature gradients of $0.03^{\circ}\text{C}/\text{km}$ or smaller, the modal temperature decreases and the standard deviation increases. A weaker gradient limit would therefore move the PF into colder waters, i.e., slightly to the north, and broaden the frontal region.

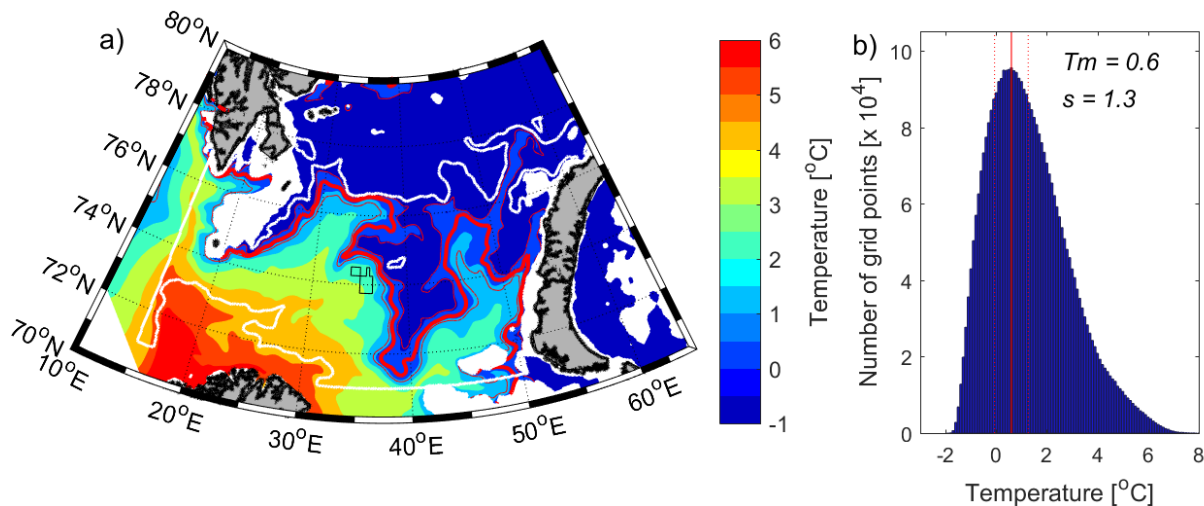


Figure 4: a) Mean temperature (colors) in the SVIM archive, 1960-2016, 50-100 m depth. Red lines show the position of the PF (thick red line T_m ; thin red lines $T_m \pm s/2$), and the white contour confines the domain, i.e., the region where temperatures are between 0.5°C and 3.5°C at least once within the hindcast period. Regions shallower than 100 m are shown in white. License PL859 is indicated in black. b) Probability density function of all temperatures from SVIM grid points with gradients exceeding 0.05°C/km based on monthly data 1960-2016. The solid and dashed red lines show T_m and $T_m \pm s/2$, respectively.

Note that when the overall mean position of the PF is examined (e.g., Figure 4), all data 1960-2016 are considered. When seasonal variations are assessed, only data for the given month are evaluated, e.g., only January data, 1960-2016, are evaluated when finding T_m and s for January (e.g., Figure 5 a,b). For interannual variations, T_m and s are calculated for each year, and all months for the given year are assessed (e.g., Figure 5 c,d).

Table 1: Temperature gradient criteria with corresponding PDF modal temperature, standard deviation, and mean number of grid points for each timestep for SVIM (monthly mean; 1960-2016) and NSA (annual mean; 1960-2012). The applied gradient criteria of 0.05°C/km is highlighted in bold.

SVIM							
T-gradient [°C/km]	0.02	0.03	0.04	0.05	0.06	0.07	0.08
T_m [°C]	0.30	0.30	0.60	0.60	0.60	0.60	0.60
s [°C]	1.66	1.55	1.38	1.33	1.28	1.25	1.22
Mean # grid points	17929	11885	8007	5439	3705	2527	1720
Nordic Seas Atlas							
T-gradient [°C/km]	0.02	0.03	0.04	0.05	0.06	0.07	0.08
T_m [°C]	1.20	1.20	1.20	1.20	0.30	0.30	0.50
s [°C]	1.26	1.31	1.29	1.27	1.09	0.97	0.94
Mean # grid points	697	274	106	45	24	16	11

4 Results

4.1 Position of physical polar front

Based on the SVIM archive, 1960-2016, the modified method of Oziel et al. (2016) identifies the mean PF along the southern edge of the Spitsbergen Bank, continuing north to the southern edge of the Great Bank, before turning southward along the western edge of the Central Bank (Figure 1), in agreement with e.g., Johannessen & Foster (1978). The front typically continues south to almost 71°N before turning northeast toward Novaya Zemlya, however, the front is less confined in the eastern Barents Sea. West of 30°E, the PF outlined in the management plan corresponds well with the front presented herein. East of 30°E, however, the front in the management plan quickly turns south and does not follow the bathymetry along the Great Bank and Central Bank. The front in the management plan is not defined east of 37°E.

4.1.1 Seasonal variability and long-term change

The southernmost position of the PF (i.e., $T_{m+s/2}$) is relatively well confined throughout the year with only small seasonal variations (Figure 5a), particularly south of the Spitsbergen Bank, Great Bank and Central Bank. Some variability is found northwest of the Spitsbergen Bank and southwest of the Novaya Zemlya Bank. Although the front appears stationary throughout the year, the temperature characteristics of the front vary (Figure 5b). The front has highest mean temperature in fall (October; 1.8°C) and lowest temperature in winter (April; -0.5°C). The temperature standard deviation is similar throughout the year.

Interannual variations in the southernmost position of the PF are generally small west of 45°E, particularly south of the Spitsbergen Bank (Figure 5c). Largest variability coincides with the regions with largest seasonal variability, i.e., southwest of the Novaya Zemlya Bank. Overall, the PF displays a slight northward trend since 1960. The northward trend is associated with a significant warming of the front (Figure 5d), consistent with an observed atlantification of the Barents Sea (Årthun et al., 2012).

License PL859 is situated southwest of the PF in a region where the PF is relatively stationary (Figure 5). The minimum distance from Korp fjell to the PF (i.e., $T_{m+s/2}$) is, however, slightly smaller in winter (on average 38 km in March) compared to summer (51 km in August and September; Figure 6a). The interannual variability is similar throughout the year, but smallest in October and with slightly enhanced values from May to July. As indicated for the annual mean values in Figure 5c, the distance from Korp fjell to the PF has increased since 1960. The increase is largest in March-June, with a total change of 10-15 km since 1960, i.e. about 2 km/decade (Figure 6b).

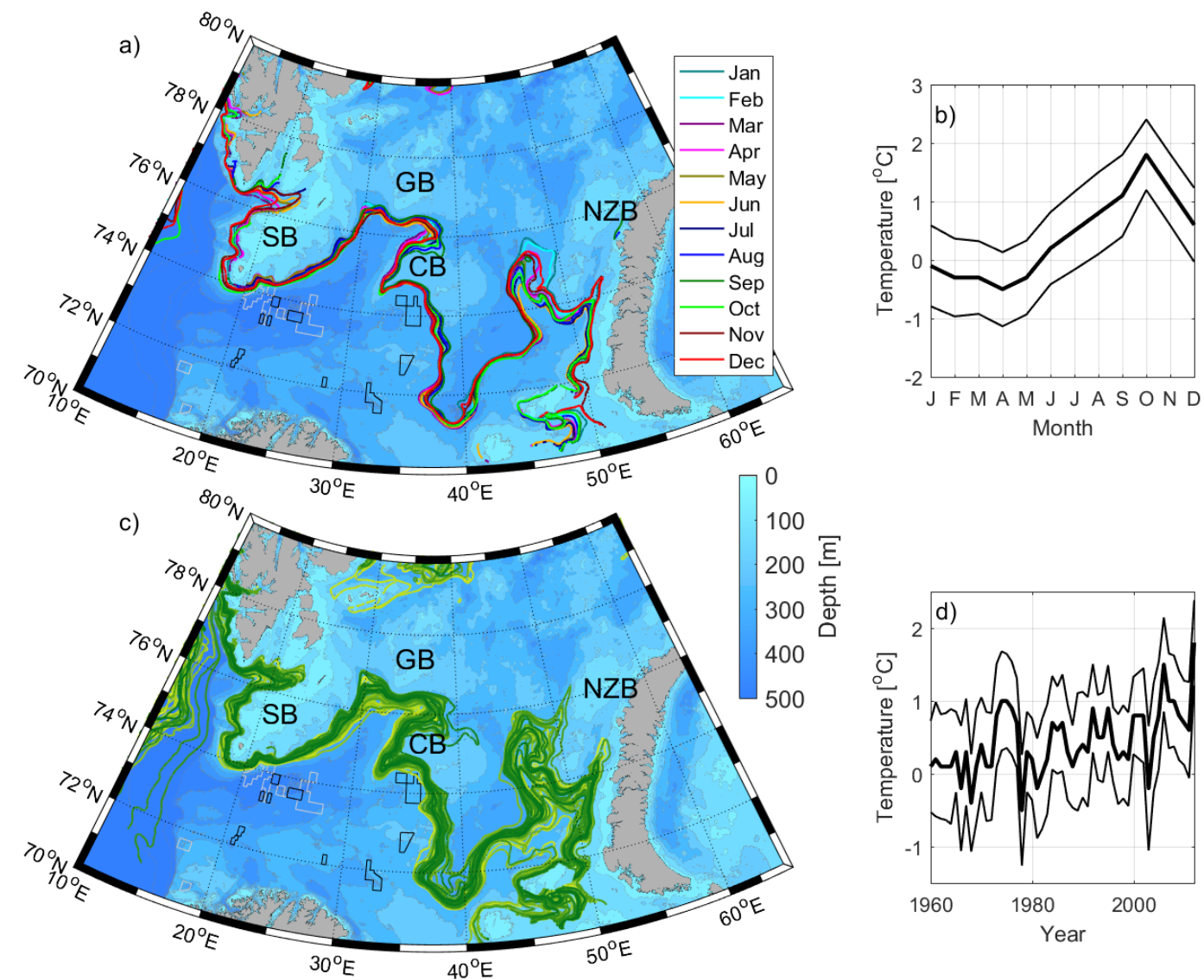


Figure 5: Monthly mean (a) and annual mean (c) southernmost position ($T_{m+s/2}$) of the PF in the SVIM archive, 1960-2016. Color contours in c) indicate time evolution from 1960 (yellow) to 2016 (green). Licenses awarded in the 23rd and 24th concession round are shown in black and white, respectively. Abbreviations are SB: Spitsbergen Bank, CB: Central Bank, GB: Great Bank, NZB: Novaya Zemlya Bank. Monthly mean (b) and annual mean (d) temperature of the PF (thick line; T_m) and its maximum and minimum temperatures (thin; $T_{m\pm s/2}$).

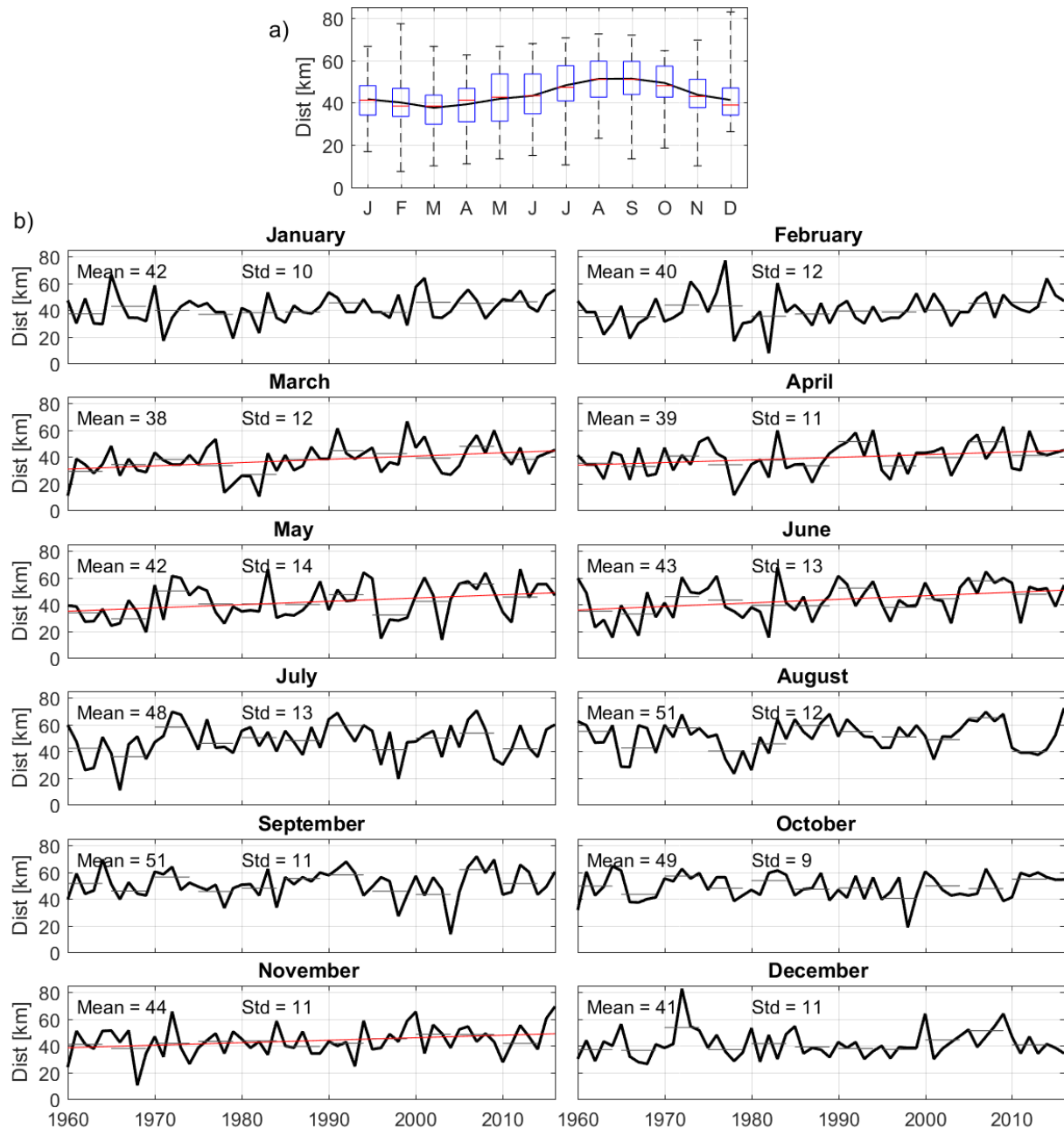


Figure 6: Seasonal variations (a) and monthly evolution (b) of the shortest distance from Korpjell to the PF, 1960-2016. The boxplot in a) indicates the median (red horizontal lines), 25 and 75 percentiles (bottom and top of blue boxes), and the maximum and minimum values (whiskers). Red lines in b) show statistically significant trends (trends that are not significant at the 95% confidence level are not shown), and horizontal grey lines show 5-year means. Mean distances and standard deviations (Std) are indicated.

4.1.2 Surface polar front

The method proposed by Oziel et al. (2016) identifies the PF by horizontal temperature gradients at 50-100 m depth. Here, we apply Oziel et al. (2016)'s method on the 0-20m upper layer in SVIM to examine variations in surface temperature gradients. The mean horizontal temperature gradients in the upper 20 m are similar to the gradients at 50-100 m depth, both in magnitude and in spatial extent (not shown). Based on the temperatures in the grid points where the temperature gradient exceeds the threshold of 0.5°C/km, the PDF has a modal temperature of 0.5°C, compared to 0.6°C for the 50-100 m layer, and the standard deviation increases from 1.3°C in the 50-100 m layer to 1.6°C in the surface layer.

The mean position of the surface PF follows the bathymetry around the Spitsbergen, Great, and Central banks (Figure 7), resembling the front defined at 50-100m depth (compare Figure 1 and Figure 7). In agreement with the 50-100 m front, the surface front deviates from the front as defined in the management plan east of 30°N, and it does not intersect with license PL859. The front is, however, less spatially confined at the surface compared to at 50-100 m depth. The surface front displays an increased seasonal cycle, both in spatial extent and temperature; in winter the 50-100 m and the 0-20 m fronts align, whereas the mean surface front typically moves northward to 76°N between the Great Bank and the Novaya Zemlya Bank in summer and warms to about 3°C (not shown). We find that the minimum distance from the surface front to Korpjell is 38 km in May and increases to 170 km in August. Also the interannual variability is enhanced at the surface, particularly east of the Central Bank (Figure 7).

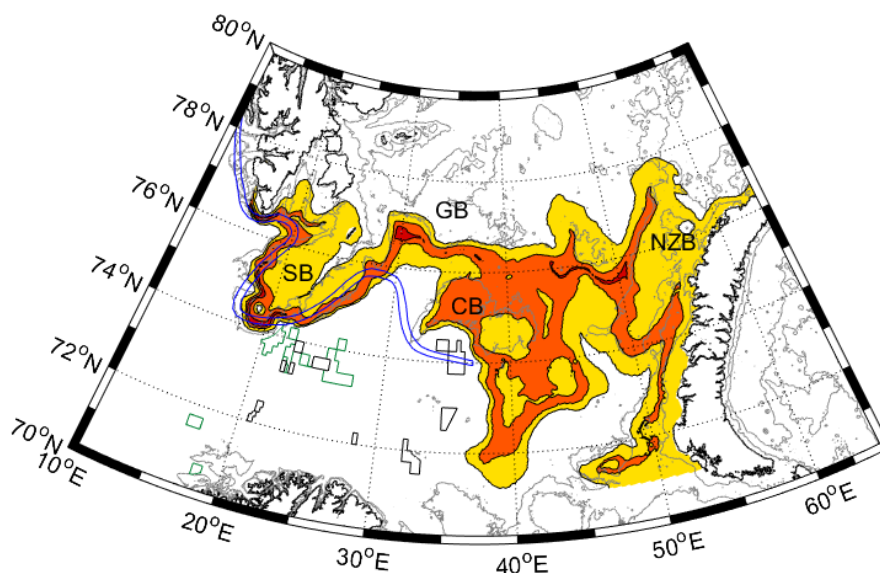


Figure 7: The 10 (yellow), 50 (orange), and 90 (red) percentiles for the location of the surface (0-20 m depth) PF in the 57-year SVIM archive. The PF as defined in the management plan (blue), licenses awarded in the 23rd (black) and 24th (green) concession round, and the 100-m and 200-m isobaths (grey) are shown. Abbreviations are SB: Spitsbergen Bank, CB: Central Bank, GB: Great Bank, NZB: Novaya Zemlya Bank.

The differences between the surface and 50-100 m layer PF positions may be related to ocean stratification; whereas the Barents Sea is well mixed in winter, the ocean becomes stratified in summer when the sea ice melts and forms a stable fresh surface layer. The positions of the PF at the surface and at 50-100 m depth are

thus aligned in winter when the ocean is well mixed, but separated in summer when the gradually more stratified waters allow for increased atmospheric warming of the surface waters.

4.2 Validation

4.2.1 Comparison with NSA

In order to evaluate the results obtained based on the SVIM archive, we examine observed annual mean temperatures at 50-100 m depth from the NSA. As the number of available observations in NSA varies greatly from year to year (Korablev et al., 2014), we consider the mean position of the PF in the NSA, but not seasonal or interannual variability. For a more detailed description of the dataset, see Korablev et al. (2014).

Although temperature gradients are generally weaker in NSA compared to SVIM (Figure 3), the positions of the strongest gradients are in good agreement. Table 1 shows that for temperature gradients below 0.06°C/km, the frontal zone is associated with higher temperatures in NSA compared to SVIM. The NSA is, however, known to have a bias toward the summer months, i.e., higher temperatures, due to better data coverage in June-September (Korablev et al., 2014; Figure 8a). For stronger temperature gradient criteria, the NSA modal temperature decreases, but very few grid points are then considered.

The mean position of the PF, calculated from the modified method of Oziel et al. (2016), is similar based on NSA and SVIM (Figure 8). In both cases the front follows the east side of the Spitsbergen Bank toward the southern side of the Great Bank, before turning south toward the Central Bank, contrasting the PF indicated in the management plan. The deviations between the PF defined by NSA and SVIM data increase in the eastern Barents Sea. We note that the observational data coverage in this region is sparse and that the data quality is poorer (Korablev et al., 2014). Note also that the positions of the fronts are similar near license PL859 although the NSA PF crosses the Central Bank, whereas the SVIM PF follows the bathymetry.

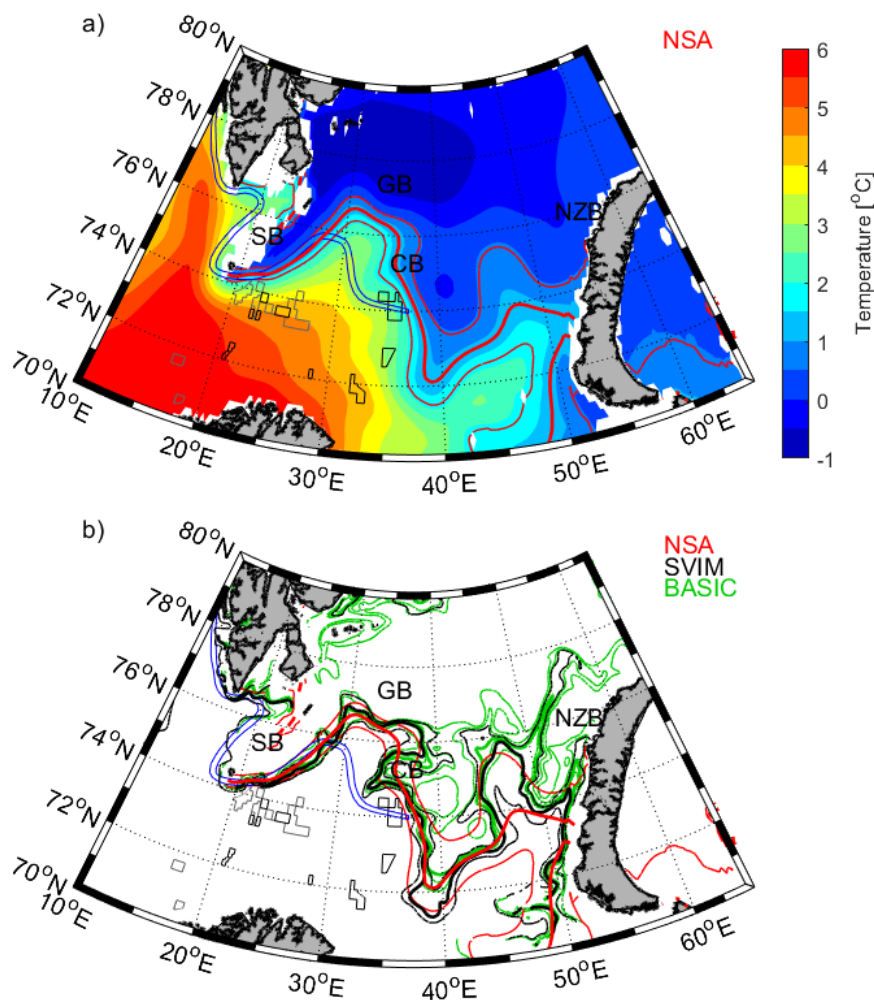


Figure 8: a) Mean temperature in NSA at 50-100 m depth, 1960-2012 (colors) and the mean position of the PF (T_m , thick; $T_m \pm s/2$, thin) in NSA. b) The mean position of the PF (T_m , thick; $T_m \pm s/2$, thin) in NSA (red), SVIM (black), and BaSIC4 (green). The PF as defined in the management plan (blue), and licenses awarded in the 23rd (black) and 24th (grey) concession round are indicated.

4.2.2 Comparison with BaSIC4

To evaluate the results based on SVIM, the method modified from Oziel et al. (2016) has also been applied on the BaSIC4 hindcast (Røed et al., 2015), i.e., a 31 year-long (1982-2012) hindcast employing ROMS coupled to an ice model and forced with NORA10. The hindcast is run on a 4 km × 4 km grid and covers the Nordic Seas, Barents Sea, North Sea, and the northeast Atlantic Ocean south to about 50°N. BaSIC4 reproduces the currents in the Barents Sea Opening fairly to very well, but the temperature and salinity in the Barents Sea are generally biased high, possibly due to too weak cross shelf mixing (Røed et al., 2015). For a more detailed description of the dataset, see Røed et al. (2015).

The mean position of the BaSIC4 PF agrees well with the SVIM PF, and they practically overlap west of 38°N (Figure 8b). In agreement with SVIM, the BaSIC4 hindcast shows small seasonal variations, but slightly shorter distance from license PL859 to the PF in winter (34 km in March; not shown) compared to summer (57 km in August). This may not be surprising as the BaSIC4 and SVIM hindcasts both employ ROMS coupled to an ice model, and are forced with NORA10. There are no statistically significant trends in the distance from Korp fjell to the PF based on the BaSIC4 archive, 1982-2012. We note that also in SVIM, trends are not significant over the shorter period (not shown).

5 Summary and conclusions

Based on a 57-year hindcast archive (SVIM), we find that the physical polar front (PF) in the Barents Sea appears relatively stationary; it has small seasonal variations, and only small interannual and long-term changes since 1960. The front follows the bathymetry south of the Spitsbergen, Great, and Central banks, before continuing east toward the Novaya Zemlya Bank. Southwest of the Novaya Zemlya Bank, however, the variability increases, both on seasonal and interannual timescales. The management plan shows a stationary front following the Spitsbergen Bank before quickly turning south at 30°E. The PF based on SVIM data thus diverges from the management plan at 30°E. The mean position of the SVIM PF is, however, supported by an observational dataset (NSA; 1960-2012) and a model hindcast (BaSIC4, 1982-2012).

Special emphasis is put on Korp fjell Deep (the planned well 7335/3-1 in license PL859), as PL859 intersects with the PF as defined in the management plan. Based on SVIM, NSA, and BaSIC4 we find, however, that PL859 is located southwest of the PF in a region where the PF shows little variability. The minimum distance between the PF and well 7335/3-1 increases from 38 km in March to 51 km in August and September, and has shifted 10-15 km northeastward in winter and spring since 1960. The trend is associated with a warming of the front, in agreement with the recent observed warming of the Barents Sea. Based on the SVIM archive, we find that the Barents Sea PF largely follows the bathymetry throughout the Barents Sea and appears relatively stationary near PL859.

6 References

- Budgell, W. P. (2005). Numerical simulation of ice-ocean variability in the Barents Sea region. *Ocean Dynamics*, 370–387.
- Drinkwater, K., & Tande, K. (2013). Biophysical studies of the Polar Front in the Barents Sea and the Arctic. *Journal of Marine Systems*, 131-133.
- Gammelsrød, T., Leikvin, Ø., Lien, V., Budgell, W., Loeng, H., & Maslowski, W. (2009). Mass and heat transports in the NE Barents Sea: Observations and models. *Journal of Marine Systems*, 56-69.
- Ingvaldsen, R. B. (2005). Width of the North Cape Current and location of the Polar Front in the western Barents Sea. *Geophysical Research Letters*, L16603.
- Ingvaldsen, R. B., Asplin, L., & Loeng, H. (2004). The seasonal cycle in the Atlantic transport to the Barents Sea during the years 1997-2001. *Continental Shelf Research*, 1015-1032.
- Johannessen, O., & Foster, L. (1978). A note on the topographically controlled oceanic polar front in the Barents Sea. *Journal of Geophysical Research*, 4567-4571.

-
- Korablev, A., Smirnov, A., & Baranova, O. (2014). *Climatological Atlas of the Nordic Seas and Northern North Atlantic*. NOAA Atlas NESDIS 77.
- Lien, V., Gusdal, Y., Albrechtsen, J., Melsom, A., & Vikebø, F. (2013). *Evaluation of a Nordic Seas 4 km numerical ocean model archive*. Fisken og Havet.
- Loeng, H. (1991). Features of the physical oceanographic conditions in the Barents Sea. *Polar Research*, 5-18.
- MET Norway Thredds Service. (2017). <http://thredds.met.no/thredds/catalog/nansen-legacy-ocean/SVIM/catalog.html>.
- Midttun, L., & Loeng, H. (1986). *Climatic variations in the Barents Sea*. The effect of oceanographic conditions on distribution and population dynamics of commercial fish stocks in the Barents Sea.
- Ministry of Climate and Environment. (2006). *St.meld. nr. 8: Helhetlig forvaltning av det marine miljø i Barentshavet og havområdene utenfor Lofoten (forvaltningsplan)*. Miljøverndepartementet.
- Ministry of Climate and Environment. (2011). *Meld. St. 10. Oppdatering av forvaltningsplanen for det marine miljø i Barentshavet og havområdene utenfor Lofoten*. Klima- og miljødepartementet.
- Oziel, L., Sirven, J., & Gascard, J.-C. (2016). The Barents Sea frontal zones and water masses variability (1980–2011). *Ocean Science*, 169-184.
- Parsons, A. R., Bourke, R. H., Muench, R. D., Chiu, C.-S., Lynch, J. F., Miller, J. H., . . . Pawlowicz, R. (1996). The Barents Sea Polar Front in summer. *Journal of Geophysical Research*, 14201-14221.
- Reistad, M., Breivik, Ø., Haakenstad, H., Aarnes, O., Furevik, B., & Bidlot, J. (2011). A high-resolution hindcast of wind and waves for the North. *Journal of Geophysical Research*, C05019.
- Røed, L., Lien, V., Melsom, A., Kristensen, N., Gusdal, Y., Ådlandsvik, B., & Albrechtsen, J. (2015). *BaSIC Technical Report 4, Part I: Evaluation of the BaSIC4 long term hindcast results*. Norwegian Meteorological Institute.
- Shchepetkin, J., & McWilliams, J. (2005). The regional oceanic modeling system (ROMS): a split-explicit, free-surface, topography-following-coordinate oceanic model. *Ocean Modelling*, 347-404.
- Statoil ASA. (2018, 03 07). Retrieved from Søknad om tillatelse til virksomhet etter forurensingsloven for boring av letebrønnene 7324/3-1 Intrepid Eagle, 7335/3-1 Korpjell Deep og 7132/2-1 Gjøkåsen: <http://www.miljodirektoratet.no/Documents/Skjema/Soknad%20om%20boring%20av%20letebronnene%20Intrepid%20Eagle%20Korpjell%20Deep%20og%20Gjokasen.pdf>
- Årthun, M., Eldevik, T., Smedsrud, L., Skagseth, Ø., & Ingvaldsen, R. (2012). Quantifying the Influence of Atlantic Heat on Barents Sea Ice Variability and Retreat. *Journal of Climate*, 4736-4743.